Robust adaptive neuronal controller for exoskeletons with sliding-mode

Ayoub Jebri, Tarek Madani, K. Djouani, Abdelaziz Benallegue

Version of Record: https://www.sciencedirect.com/science/article/pii/S0925231220302848
Manuscript_8561086b3bc2f6a3f70f27a8bac6c091

Robust Adaptive Neuronal Controller for Exoskeletons with Sliding-Mode

A. Jebri, T. Madani, K. Djouani, and A. Benallegue

Ayoub Jebri (ayoub.jebri@u-pec.fr), Tarek Madani (tarek.madani@u-pec.fr) and Karim Djouani (djouani@u-pec.fr), are with Laboratoire Images, Signaux et Systemes Intelligents, University Paris-Est Créteil, 94400 Vitry sur Seine, France.

Karim Djouani (DjouaniK@tut.ac.za) is also with French South African Insitute of Technology (F'SATI), Tshwane University of Technlogy, Pretoria, South Africa.

Abdelaziz Benallegue (benalleg@lisv.uvsq.fr) is with Laboratoire d'Ingénierie des Systèmes de Versailles, UVSQ, Université Paris-Saclay, 78140 Velizy, France.

Abstract

A robust neural adaptive integral sliding mode control approach is proposed in this present paper to deal with the nonlinear exoskeleton systems. The proposed control technique is composed of two parts: an adaptive neural network controller and an adaptive integral terminal sliding mode controller. The adaptive laws are developed to estimate unknown parameters in order to ensure asymptotic stability of the closed loop system. Only classical system's properties are supposed to be known, such as the bounds on some parameters. The system's dynamics are not known but are estimated on line by the neural network control part. The proposed adaptive control strategy is designed to ensure the reaching of the sliding mode with enhanced tracking performance. The singularity problem of the terminal sliding mode approach is removed without adding any constraint. The closed-loop stability of the system in the sense of Lyapunov is demonstrated. The effectiveness of the proposed approach is tested in real time application with healthy human subjects by performing passive arm movements using a 2-DOF upper limb exoskeleton.

Keywords: Adaptive control, Sliding mode, Neural network, Exoskeleton.

1. Introduction

Research and technological development in robotics have opened up new fields of application for exoskeletons. These portable robots are particularly suitable for repetitive movements with force control and human assistance. In physiotherapy applications, the patient's recovery depends on the quality of rehabilitation. This quality of rehabilitation could be improved through the use of exoskeletons [1, 2, 3]: (i) By reducing the cost of the sessions and increasing their number. (ii) By freeing up clinical staff for tasks requiring more qualification. (iii) By measuring interaction torques and forces to evaluate the patient's level of motor recovery. Generally, it is very difficult to ensure the recovery of patients who have partially or totally lost their natural movements with conventional medical treatment. Physiotherapy is often used to achieve rapid recovery of voluntary movements. This can be done through physical exercises in which an attempt is made to mobilize the affected limbs of the patient.

In the initial phase of rehabilitation, the recovery process consists mainly of passive movements of the affected limbs. Especially for this phase of therapy, the use of trajectory tracking alone is sufficient to meet the desired needs in this phase of rehabilitation. The interaction between humans and the exoskeleton is a new challenge for robotic control strategies. Indeed, misalignment and changes in dynamics cause perturbations and increase uncertainties. Different control strategies have been proposed to deal with this, such as PID control [4], sliding mode control [5] or neural network control [6].

The ability of neural networks (NN) to approach complex non-linear functions makes them a major tool for improving conventional control loops [7]. For non-linear and time-varying systems, NNs have shown their effectiveness in control loops [8, 9]. Therefore, exoskeletons with their changing and non-linear dynamics are good candidates to be approached by NN. Different types of NN have been proposed to construct non-linear dynamic estimators or control non-linear systems, such as the radial basis function NN [10] or the Multi-Layer Perceptron NN [11].

The Sliding Mode (SM) technique, with its robustness to external disturbances and parametric variations, is an effective control solution to manage uncertainties and reject disturbances. The sliding mode controller drives the trajectory error to an defined sliding surface. Then, the switching phenomenon maintains this trajectory on the surface to slide it towards zero.

Conventional sliding mode methods allow asymptotic convergence of the error [12]. Other techniques improve the convergence of the tracking error to zero, such as the terminal sliding mode [13] and the fast terminal sliding mode [14]. These last suffer from singularity problems due to the use of fractional power in sliding surface design. Afterward, various strategies have been developed in order to propose methods to overcome the singularity problem, such as the non-singular terminal sliding mode control [5, 15, 16] and the integral terminal sliding mode [17, 18, 19].

The combination of the NN and SM techniques is of interest for the controller design for nonlinear systems with uncertainties, as for instance the exoskeletons. In [10], the authors present an adaptive NN controller for robots based on the terminal sliding mode methodology. However, the problem of singularity in the control law has not been resolved. This problem can cause very large power level demands that the control organ will not be able to provide. In this paper, a new adaptive controller based on NN and SM is proposed ensuring that the singularity problem is completely avoided. Furthermore, the knowledge of the dynamic model is not required for the proposed controller. The dynamic of the exoskeleton-human system is governed by several complex effects, such as inertia, Coriolis and friction [20, 21]. Only some classical properties of the model are assumed to be known for designing the controller such as the limitation of human torques or the boundedness of the desired trajectories [18, 19]. The NN are used to compensate for the nonlinear dynamics of the exoskeleton-human system in real time. The proposed NN learning algorithm is unsupervised, which leads to avoiding the offline learning database. A stable closed-loop algorithm is proposed to update the adaptive NN and SM parameters and to ensure the tracking of the desired trajectories. The closed-loop system stability is demonstrated with the Lyapunov theorem. Experiments are conducted on an upper limb exoskeleton named ULEL[1] to illustrate the effectiveness of the proposed approach.

In the rest of this article, section 2 presents the system with the dynamic model and neural approximation. In section 3, the control strategy and sliding surface are presented. Stability is discussed in Section 4. Section 5 presents the results of the experiment, where all rehabilitation tasks are performed with healthy subjects. Finally, Section 6 is a conclusion of this work.

[1]Upper Limb Exoskeleton of LISSI

2. System modeling

2.1. Dynamic model

The system considered is formed by the exoskeleton and the wearer. The dynamic model resulting from Euler-Lagrange formalism is expressed in vector form as follows

$$M(q)\,\ddot{q} + C(q,\dot{q})\dot{q} + G(q) + D(\dot{q}) = u + \tau^{hum} + \tau^{ext}, \tag{1}$$

where $q \in \mathbb{R}^n$, $\dot{q} \in \mathbb{R}^n$, $\ddot{q} \in \mathbb{R}^n$ are respectively position, velocity and acceleration of the joints; $M(q) \in \mathbb{R}^{n\times n}$ is the inertia matrix of the system; $C(q,\dot{q}) \in \mathbb{R}^{n\times n}$ is the Coriolis and centrifugal matrix; $G(q) \in \mathbb{R}^n$ is a vector containing all the terms related to gravity forces; $D(\dot{q}) \in \mathbb{R}^n$ is a vector containing the dissipation terms; $\tau^{hum} \in \mathbb{R}^n$ is a vector of the human torques; $\tau^{ext} \in \mathbb{R}^n$ is a vector of external disturbance torques and $u \in \mathbb{R}^n$ is a vector of exoskeleton torques applied at the joints.

The system under consideration (1) is only composed of pivot joints. Therefore, the following useful properties are verified for $q \in \mathbb{R}^n$.

Property 1: The matrix $M(q)$ is bounded symmetric positive-definite [22]

$$c_{M1}\,||x||^2 \leq x^T M(q)\,x \leq c_{M2}\,||x||^2 \ , \ \forall x \in \mathbb{R}^n, \tag{2}$$

where c_{M1} and c_{M2} are positive constants.

Property 2: The matrix $C(q,\dot{q})$ can always be chosen so that $[\dot{M}(q) - 2C(q,\dot{q})]$ is skew symmetric, so we can write

$$\frac{1}{2}\,x^T[\dot{M}(q) - 2\,C(q,\dot{q})]\,x = 0, \ \forall x \in \mathbb{R}^n. \tag{3}$$

2.2. Neuronal approximation

Some parameter variations, such as a change of user, lead to a change in the system dynamics. To counteract these variations, an adaptive method using neural networks was chosen to address these changes in dynamics. All non-linear functions representing the elements of the matrices $M(q)$, $C(q,\dot{q})$, $G(q)$ and $D(\dot{q})$ are considered unknown. Three-layer Neural Networks (MLPNN) are used to approximate these non-linear functions [23, 24, 25].

The MLPNN is of the form $W_2^T\,\Phi(W_1^T\,X)$, with W_1, W_2 are the synaptic weight matrices of the hidden and output layer respectively, X is the input vector variable and Φ is the sigmoidal activation function of the hidden layer.

The activation function of the output layer is linear. The nonlinear functions $M(q)$, $C(q,\dot{q})$, $G(q)$ and $D(\dot{q})$ are written as

$$\begin{cases} M(q) = W_{2M}^T \Phi_M(W_{1M}^T X_M(q)) + \varepsilon_M(q) \\ C(q,\dot{q}) = W_{2C}^T \Phi_C(W_{1C}^T X_C(q,\dot{q})) + \varepsilon_C(q,\dot{q}) \\ G(q) = W_{2G}^T \Phi_G(W_{1G}^T X_G(q)) + \varepsilon_G(q) \\ D(\dot{q}) = W_{2D}^T \Phi_D(W_{1D}^T X_D(\dot{q})) + \varepsilon_D(\dot{q}) \end{cases} \tag{4}$$

where $\varepsilon_M(q)$, $\varepsilon_C(q,\dot{q})$, $\varepsilon_G(q)$ and $\varepsilon_D(\dot{q})$ are the neural network approximation errors.

- The input variables of the neural networks are given by

$$\begin{aligned} X_M(q) &= I \otimes q \in \mathbb{R}^{n^2 \times n}, \\ X_C(q,\dot{q}) &= I \otimes \begin{bmatrix} q \\ \dot{q} \end{bmatrix} \in \mathbb{R}^{2n^2 \times n}, \\ X_G(q) &= q \in \mathbb{R}^n, \\ X_D(\dot{q}) &= \dot{q} \in \mathbb{R}^n, \end{aligned} \tag{5}$$

  with $\otimes$ is the Kronecker product and $I \in \mathbb{R}^{n \times n}$ is the identity matrix.

- The optimal synaptic weight matrices are given by

$$
\begin{aligned}
W_{1M} &= \begin{bmatrix} W_{1M,1} & & 0 \\ & \ddots & \\ 0 & & W_{1M,n} \end{bmatrix} \in \mathbb{R}^{n^2 \times n\, p_M}, \\
W_{2M} &= \begin{bmatrix} W_{2M,1} \\ \vdots \\ W_{2M,n} \end{bmatrix} \in \mathbb{R}^{n\, p_M \times n}, \\
W_{1C} &= \begin{bmatrix} W_{1C,1} & & 0 \\ & \ddots & \\ 0 & & W_{1C,n} \end{bmatrix} \in \mathbb{R}^{2\, n^2 \times n\, p_C}, \\
W_{2C} &= \begin{bmatrix} W_{2C,1} \\ \vdots \\ W_{2C,n} \end{bmatrix} \in \mathbb{R}^{n\, p_C \times n}, \\
W_{1G} &\in \mathbb{R}^{n \times p_G},\ W_{2G} \in \mathbb{R}^{p_G \times n}, \\
W_{1D} &\in \mathbb{R}^{n \times p_D},\ W_{2D} \in \mathbb{R}^{p_D \times n},
\end{aligned}
\tag{6}
$$

  where $W_{1M,i} \in \mathbb{R}^{n \times p_M}$, $W_{2M,i} \in \mathbb{R}^{p_M \times n}$, $W_{1C,i} \in \mathbb{R}^{2\, n \times p_C}$, $W_{2C,i} \in \mathbb{R}^{p_C \times n}$ for $i = 1, ..., n$ and p_M, p_C, p_G, $p_D \in \mathbb{N}$ are the number of neurons in the hidden layer for $M(q)$, $C(q, \dot{q})$, $G(q)$ and $D(\dot{q})$ respectively.

- The sigmoidal activation functions, item-by-item, of the hidden layers are given by

$$
\begin{aligned}
&\Phi_M(W_{1M}^T X_M) \in \mathbb{R}^{n\, p_M \times n}, \\
&\Phi_C(W_{1C}^T X_C) \in \mathbb{R}^{n\, p_C \times n}. \\
&\Phi_G(W_{1G}^T X_G) \in \mathbb{R}^{p_G}, \\
&\Phi_D(W_{1D}^T X_D) \in \mathbb{R}^{p_D}.
\end{aligned}
\tag{7}
$$

For simplicity of presentation, the arguments (q), $(\dot{q})$ and $(q, \dot{q})$ are omitted in the rest of this paper. Furthermore, a generic matrix N will be used to

represent the matrices to be estimated M, C, G and D such as

$$N = W_{2N}^T \Phi_N(W_{1N}^T X_N) + \varepsilon_N, \tag{8}$$

with $N \in \{M, C, G, D\}$.

These optimal networks $N \in \{M, C, G, D\}$ (8) are approximated by $\hat{N} \in \{\hat{M}, \hat{C}, \hat{G}, \hat{D}\}$

$$\hat{N} = \hat{W}_{2N}^T \Phi_N(\hat{W}_{1N}^T X_N), \tag{9}$$

where $\hat{W}_{1N}$ and $\hat{W}_{2N}$ are the estimations of W_{1N} and W_{2N} respectively.

The adaptation laws of the weights $\hat{W}_{1N}$ and $\hat{W}_{2N}$, will be given in the stability section.

Before introducing the proposed controller, let introduce the following assumptions in relation to the neural approximations:

Assumption 1 : The matrices of optimal synaptic weights W_{1N} and W_{2N} are bounded:

$$||W_{1N}||_F \leq c_{W_{1N}}, \; ||W_{2N}||_F \leq c_{W_{2N}}, \tag{10}$$

where $c_{W_{1N}}$ and $c_{W_{2N}}$ are positive constantes and $||.||_F$ is the Frobenius norm[2].

Assumption 2 : The approximation error of the optimal neural networks $\varepsilon_N(X_N)$ are bounded:

$$||\varepsilon_N||_F \leq c_{\varepsilon_N}, \tag{11}$$

where c_{ε_N} is a positive constant.

3. Controller design

In this section, an adaptive NN and SM controller is proposed for the considered system (1). The main objective is to ensure the tracking of the desired trajectories $q_d(t) \in \mathbb{R}^n$. The control law is developed in two steps: Firstly, a nonsingular integral terminal sliding surface is selected. Secondly, an adaptive control law is designed. The NN approximation is combined with the SM technique to compensate for the deviation due to the approximation errors and the robustness of the closed-loop system against external perturbation.

[2]Frobenius norm of x is define by $\|x\|_F = \sqrt{tr(x^T x)}$.

3.1. Switching law selection

Let the position error be the variable $e(t) \in \mathbb{R}^n$, such as

$$e(t) = q_d(t) - q(t). \tag{12}$$

To avoid any singularity problem, the ITSM (Integral Terminal Sliding Mode) switching law is chosen in this work. The selected switching law [26] is given by [3]

$$s(t) = \dot{e}(t) + \alpha \int_0^t e^{\gamma_1}(\mu)\, d\mu + \beta \int_0^t \dot{e}^{\gamma_2}(\mu)\, d\mu + \eta, \tag{13}$$

where $\gamma_1 = \frac{q}{2p-q}$ and $\gamma_2 = \frac{q}{p}$ with p and q are odd positive integers such as $p > q > 0$; $\alpha = diag(\alpha_1, ..., \alpha_n) \in \mathbb{R}^{n\times n}$ and $\beta = diag(\beta_1, ..., \beta_n) \in \mathbb{R}^{n\times n}$ are positive constant diagonal matrices chosen such as polynomials $r^2 + \beta_i r + \alpha_i$ for $i = 1, ..., n$ are Hurwitz; $\eta \in \mathbb{R}^n$ is a constant vector that can be chosen $\eta = -\dot{e}(0)$ to obtain $s(0) = 0$ (initial condition on the sliding surface).

The time derivative of equation (13) lead to

$$\dot{s} = \ddot{e} + \alpha\, e^{\gamma_1} + \beta\, \dot{e}^{\gamma_2}. \tag{14}$$

Remark: For the control law synthesis, the switching law s is differentiated with respect to time. In Terminal Sliding Mode or Fast Terminal Sliding Mode switching law [27], the terms $e^{\gamma_1 - 1}$ or $\dot{e}^{\gamma_2 - 1}$ emerge in the derivative of s. The negative powers $(\gamma_1 - 1)$ and $(\gamma_2 - 1)$ of these terms make singularities for null position or velocity errors. The presence of the integral in the proposed sliding surface prevents the occurrence of singularity in the derivative. For the proposed sliding surface (13), it is notable from the equation (14) that $\dot{s}$ is defined for all e, $\dot{e}$ and $\ddot{e} \in \mathbb{R}^n$.

Using equations (1), (12) in (14), we get

$$\dot{s} = \ddot{q}_d - M^{-1}(u + \tau_{hum} + \tau_{ext} - C\,\dot{q} - G - D) + \alpha\, e^{\gamma_1} + \beta\, \dot{e}^{\gamma_2}. \tag{15}$$

Multiplying both sides of the equation (15) by the matrix M

$$M\,\dot{s} = M\,(\ddot{q}_d + \alpha\, e^{\gamma_1} + \beta\, \dot{e}^{\gamma_2}) - u - \tau_{hum} - \tau_{ext} + C\,\dot{q} + G + D. \tag{16}$$

[3] The notation x^γ for $x \in \mathbb{R}^n$ $x^\gamma = [x_1^\gamma, ..., x_n^\gamma]^T$.

After few arrangements the previous equation (16) can be expressed as

$$M\,\dot{s} + Cs = M\,\ddot{q}_r + C\,\dot{q}_r + G + D - \tau_{hum} - \tau_{ext} - u, \tag{17}$$

where $\dot{q}_r \in \mathbb{R}^n$ and $\ddot{q}_r \in \mathbb{R}^n$ are velocity and acceleration references respectively, given by

$$\begin{cases} \dot{q}_r = \dot{q} + s = \dot{q}_d + \alpha \int_0^t e^{\gamma_1}(\mu)\, d\mu + \beta \int_0^t \dot{e}^{\gamma_2}(\mu)\, d\mu + \eta \\ \ddot{q}_r = \ddot{q} + \dot{s} = \ddot{q}_d + \alpha\, e^{\gamma_1} + \beta\, \dot{e}^{\gamma_2} \end{cases} \tag{18}$$

The elements M, C, G and D are substituted by their neural estimations $\hat{M}$, $\hat{C}$, $\hat{G}$ and $\hat{D}$ respectively in the equation (17)

$$M\,\dot{s} + C\,s = (\hat{M}\,\ddot{q}_r + \hat{C}\,\dot{q}_r + \hat{G} + \hat{D}) + \xi - u, \tag{19}$$

with ξ is a vector which contains errors of neural approximation and the torques τ_{hum} and τ_{ext} such as

$$\xi = \tilde{M}\,\ddot{q}_r + \tilde{C}\,\dot{q}_r + \tilde{G} + \tilde{D} - \tau_{hum} - \tau_{ext}, \tag{20}$$

where $\tilde{(.)} = (.) - \hat{(.)}$.

In following section, a control law will be proposed to guarantee the system stability (19) by using the neural estimation part $(\hat{M}\,\ddot{q}_r + \hat{C}\,\dot{q}_r + \hat{G} + \hat{D})$ and a robust sliding mode part to compensate the unknown part ξ.

3.2. Control law conception

A control law based on NN is established to ensure the compensation of system dynamics and the convergence of trajectory tracking error through a switching manifold. For this purpose, the following additional assumptions are needed:

Assumption 3 :The boundness of the desired positions q_d, velocities $\dot{q}_d$ and accelerations $\ddot{q}_d$ are admitted

$$||q_d|| \leq c_{q_d},\ ||\dot{q}_d|| \leq c_{\dot{q}_d},\ ||\ddot{q}_d|| \leq c_{\ddot{q}_d}, \tag{21}$$

where c_{q_d}, $c_{\dot{q}_d}$ and $c_{\ddot{q}_d}$ are positive constants.

Assumption 4 : The human τ_{hum} and external τ_{ext} torques are admitted bounded

$$||\tau_{hum}|| \leq c_{\tau_{hum}},\ ||\tau_{ext}|| \leq c_{\tau_{ext}}, \tag{22}$$

where $c_{\tau_{hum}}$ and $c_{\tau_{ext}}$ are positive scalars

The sum of the two control torques u_{NN} and u_{SM} form the proposed control law u, as follow:

$$u = u_{NN} + u_{SM}, \tag{23}$$

where :

- The torque u_{NN} represent an adaptive control using the neural networks and reference variables, such as

$$u_{NN} = \hat{M}\,\ddot{q}_r + \hat{C}\,\dot{q}_r + \hat{G} + \hat{D}, \tag{24}$$

with $\hat{M}, \hat{C}, \hat{G}, \hat{D}$ the different neural networks approximators. The associated parameter adaptation rules $\hat{W}_{\{1,2\}\{M,C,G,D\}}$ will be introduced later when discussing the stability demonstration.

- The sliding mode compensation term is represented by

$$u_{SM} = \hat{\theta}^T \Psi(q, \dot{q}, \dot{q}_r, \ddot{q}_r, \hat{W})\, K\, \frac{s}{\|s\|}, \tag{25}$$

where $K \in \mathbb{R}^{n\times n}$ is a diagonal matrix formed by positive constant scalars and the vector $\Psi(q, \dot{q}, \dot{q}_r, \ddot{q}_r, \hat{W}) \in \mathbb{R}^8$ is defined, as follows

$$\Psi(q, \dot{q}, \dot{q}_r, \ddot{q}_r, \hat{W}) = \begin{bmatrix} 1 \\ ||\dot{q}_r|| \\ ||\ddot{q}_r|| \\ ||\hat{W}||_F\, ||q|| \\ ||\hat{W}||_F\, ||\dot{q}|| \\ ||\hat{W}||_F\, ||q||\, ||\dot{q}_r|| \\ ||\hat{W}||_F\, ||\dot{q}||\, ||\dot{q}_r|| \\ ||\hat{W}||_F\, ||q||\, ||\ddot{q}_r|| \end{bmatrix}, \tag{26}$$

with $\hat{W}$ the matrix containing all the parameters $\hat{W}_{\{1,2\}\{M,C,G,D\}}$ and $\hat{\theta} = [\hat{\theta}_1, ..., \hat{\theta}_8]^T \in \mathbb{R}^8$ is the estimated vector seeking to approach the positive unknown vector $\theta = [\theta_1, ..., \theta_8]^T \in \mathbb{R}^8$. The vector $\hat{\theta}$ is given by the following adaptation law (27)

$$\dot{\hat{\theta}} = \Gamma_\theta\, \Psi(q, \dot{q}, \dot{q}_r, \ddot{q}_r, \hat{W})\, ||s||. \tag{27}$$

The proposed adaptive controller scheme is illustrated in figure 1. The obtained control law is formed by two parts, corresponding to the adaptive NN control for the first part , and the adaptive SM control, for the second one.

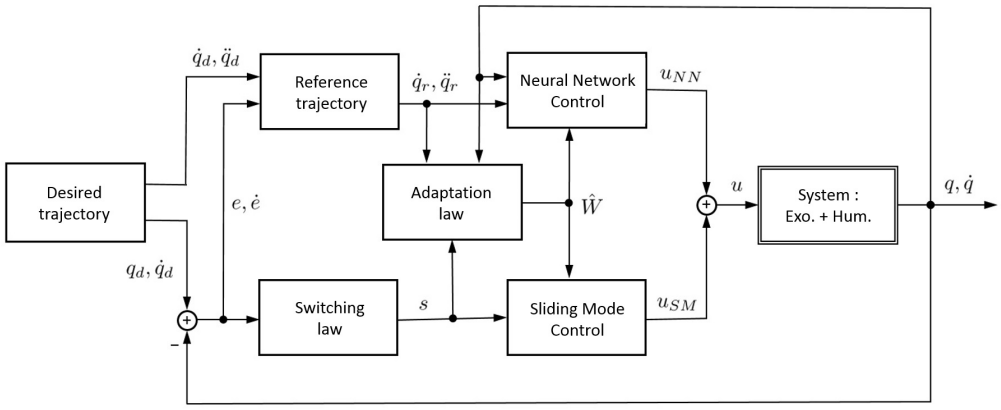

Figure 1: The proposed adaptive controller scheme

4. Stability analysis

The stability proof in Lyapunov sense of the proposed control law is given in this section. Considering that the activation functions $\Phi(W_N^T X_N)$ are nonlinear, they are approached by a first order Taylor series expansion in the neighborhood of $\hat{W}_N^T X_N$

$$\Phi(W_{1N}^T X_N) = \Phi(\hat{W}_{1N}^T X_N) + \acute{\Phi}(\hat{W}_{1N}^T X_N)\, \tilde{W}_{1N}^T X_N + O_N, \tag{28}$$

where O_N is superior order terms of the Taylor series, $\tilde{W}_{1N} = (W_{1N} - \hat{W}_{1N})$ represent approximation error and $\acute{\Phi}(\hat{W}_{1N}^T X_N)$ is the diagonal Jacobian matrix[4], such as

$$\begin{aligned} &\acute{\Phi}(\hat{W}_{1M}^T X_M) \in \mathbb{R}^{n\,p_M \times n\,p_M}, \\ &\acute{\Phi}(\hat{W}_{1C}^T X_C) \in \mathbb{R}^{n\,p_C \times n\,p_C}, \\ &\acute{\Phi}(\hat{W}_{1G}^T X_G) \in \mathbb{R}^{p_G \times p_G}, \\ &\acute{\Phi}(\hat{W}_{1D}^T X_D) \in \mathbb{R}^{p_D \times p_D}. \end{aligned} \tag{29}$$

[4]The Jacobian $\acute{\Phi}(y) = \left.\frac{\partial \Phi(x)}{\partial x}\right|_{x=y}$.

211 According to (28), it is clear that

$$O_N = \Phi(W_{1N}^T X_N) - \Phi(\hat{W}_{1N}^T X_N) - \acute{\Phi}(\hat{W}_{1N}^T X_N)\, \tilde{W}_{1N}^T X_N. \tag{30}$$

212 The sigmoidal function $\Phi(.)$ and its derivative $\acute{\Phi}(.)$ are bounded, so ac-
213 cording to assumption 1 approximation error O_N are bounded by

$$||O_N||_F \leq c_{\Delta_{N1}} + c_{\Delta_{N2}} ||\tilde{W}_{1N}||_F \, ||X_N||_F, \tag{31}$$

214 where $c_{\Delta_{N1}}$ and $c_{\Delta_{N2}}$ are positive scalar.
215 The following notations are introduced for simplicity of expression

$$\begin{cases} \Phi(W_{1N}^T X_N) = \Phi_N \\ \Phi(\hat{W}_{1N}^T X_N) = \hat{\Phi}_N \\ \acute{\Phi}(\hat{W}_{1N}^T X_N) = \acute{\hat{\Phi}}_N \end{cases} \tag{32}$$

216 Therefore, the equation (28) becomes

$$\Phi_N = \hat{\Phi}_N + \acute{\hat{\Phi}}_N \tilde{W}_{1N}^T X_N + O_N. \tag{33}$$

217 Substituting the equations (4) and (9) into the definition $\tilde{N} = (N - \hat{N})$,
218 gives:

$$\tilde{N} = (W_{2N}^T \Phi_N + \varepsilon_N) - \hat{W}_{2N}^T \hat{\Phi}_N. \tag{34}$$

219 Adding and subtracting $\hat{W}_{2N}^T \Phi_N$ in the equation (34)

$$\tilde{N} = \tilde{W}_{2N}^T \Phi_N + \hat{W}_{2N}^T \tilde{\Phi}_N + \varepsilon_N, \tag{35}$$

220 with $\tilde{W}_{2N} = (W_{2N} - \hat{W}_{2N})$ and $\tilde{\Phi}_N = (\Phi_N - \hat{\Phi}_N)$.
221 The functions Φ_N and $\tilde{\Phi}_N$ are substituting by their Taylor series (33) in
222 the equation (35)

$$\tilde{N} = \tilde{W}_{2N}^T (\hat{\Phi}_N + \acute{\hat{\Phi}}_N \tilde{W}_{1N}^T X_N + O_N) + \hat{W}_{2N}^T (\acute{\hat{\Phi}}_N \tilde{W}_{1N}^T X_N + O_N) + \varepsilon_N \ . \tag{36}$$

223 The equation (36) can be rewritten as

$$\tilde{N} = \hat{W}_{2N}^T \acute{\hat{\Phi}}_N \tilde{W}_{1N}^T X_N + \tilde{W}_{2N}^T (\hat{\Phi}_N - \acute{\hat{\Phi}}_N \hat{W}_{1N}^T X_N) + \Delta_N \ , \tag{37}$$

224 where

$$\Delta_N = \tilde{W}_{2N}^T \acute{\hat{\Phi}}_N W_{1N}^T X_N + W_{2N}^T O_N + \varepsilon_N. \tag{38}$$

The function $\hat{\dot{\Phi}}_N$ is bounded, hence the norm of Δ_N satisfies the following inequality

$$||\Delta_N||_F \leq c_{\Delta_N}||W_{1N}||_F\,||\tilde{W}_{2N}||_F\,||X_N||_F + ||W_{2N}||_F\,||O_N||_F + ||\varepsilon_N||_F, \quad (39)$$

with c_{Δ_N} as constant scalar.

The following equality is obtained from ξ (20) by replacing $\tilde{N}$ by its expression (37)

$$\begin{aligned}\xi = \; & (\hat{W}_{2M}^T\,\hat{\dot{\Phi}}_M\,\tilde{W}_{1M}^T\,X_M + \tilde{W}_{2M}^T\,(\hat{\Phi}_M - \hat{\dot{\Phi}}_M\,\hat{W}_{1M}^T\,X_M) + \Delta_M)\,\ddot{q}_r \\ & +(\hat{W}_{2C}^T\,\hat{\dot{\Phi}}_C\,\tilde{W}_{1C}^T\,X_C + \tilde{W}_{2C}^T\,(\hat{\Phi}_C - \hat{\dot{\Phi}}_C\,\hat{W}_{1C}^T\,X_C) + \Delta_C)\,\dot{q}_r \\ & +(\hat{W}_{2G}^T\,\hat{\dot{\Phi}}_G\,\tilde{W}_{1G}^T\,X_G + \tilde{W}_{2G}^T\,(\hat{\Phi}_G - \hat{\dot{\Phi}}_G\,\hat{W}_{1C}^T\,X_G) + \Delta_G) \\ & +(\hat{W}_{2D}^T\,\hat{\dot{\Phi}}_G\,\tilde{W}_{1D}^T\,X_D + \tilde{W}_{2D}^T\,(\hat{\Phi}_D - \hat{\dot{\Phi}}_D\,\hat{W}_{1D}^T\,X_D) + \Delta_D) - \tau_{hum} - \tau_{ext}.\end{aligned} \quad (40)$$

By grouping the error terms Δ_N of the equation (40),

$$\begin{aligned}\xi = \; & (\hat{W}_{2M}^T\,\hat{\dot{\Phi}}_M\,\tilde{W}_{1M}^T\,X_M + \tilde{W}_{2M}^T\,(\hat{\Phi}_M - \hat{\dot{\Phi}}_M\,\hat{W}_{1M}^T\,X_M)\,)\,\ddot{q}_r \quad , \\ & +(\hat{W}_{2C}^T\,\hat{\dot{\Phi}}_C\,\tilde{W}_{1C}^T\,X_C + \tilde{W}_{2C}^T\,(\hat{\Phi}_C - \hat{\dot{\Phi}}_C\,\hat{W}_{1C}^T\,X_C)\,)\,\dot{q}_r \\ & +(\hat{W}_{2G}^T\,\hat{\dot{\Phi}}_G\,\tilde{W}_{1G}^T\,X_G + \tilde{W}_{2G}^T\,(\hat{\Phi}_G - \hat{\dot{\Phi}}_G\,\hat{W}_{1C}^T\,X_G)\,) \\ & +(\hat{W}_{2D}^T\,\hat{\dot{\Phi}}_G\,\tilde{W}_{1D}^T\,X_D + \tilde{W}_{2D}^T\,(\hat{\Phi}_D - \hat{\dot{\Phi}}_D\,\hat{W}_{1D}^T\,X_D)\,) + Z,\end{aligned} \quad (41)$$

where

$$Z = \Delta_M\,\ddot{q}_r + \Delta_C\,\dot{q}_r + \Delta_G + \Delta_D - \tau_{hum} - \tau_{ext}. \quad (42)$$

From the previous equation, it is established that Z is bounded by

$$||Z|| \leq ||\Delta_M||_F\,||\ddot{q}_r|| + ||\Delta_C||_F\,||\dot{q}_r|| + ||\Delta_G|| + ||\Delta_D|| + ||\tau_{hum}|| + ||\tau_{ext}||. \quad (43)$$

By applying some simplifications, the inequality (43) becomes

$$\begin{aligned}||Z|| \leq \; & c_{Z1} + c_{Z2}\,||\dot{q}_r|| + c_{Z3}\,||\ddot{q}_r|| + c_{Z4}\,||\hat{W}||_F\,||q|| + c_{Z5}\,||\hat{W}||_F\,||\dot{q}|| \\ & +c_{Z6}\,||\hat{W}||_F\,||q||\,||\dot{q}_r|| + c_{Z7}\,||\hat{W}||_F\,||q||\,||\ddot{q}_r|| + c_{Z8}\,||\hat{W}||_F\,||\dot{q}||\,||\dot{q}_r||,\end{aligned} \quad (44)$$

where c_{Z1}, ..., c_{Z8} are positive constants.

To demonstrate the system stability, a Lyapunov function candidate is considered

$$V = V_1 + V_2 + V_3, \quad (45)$$

where

$$V_1 = \frac{1}{2}\, s^T M\, s, \tag{46}$$

and[5]

$$\begin{aligned} V_2 = \frac{1}{2}\,(\; & tr(\tilde{W}_{1M}^T\, \Gamma_{1M}^{-1}\, \tilde{W}_{1M}) + tr(\tilde{W}_{2M}^T\, \Gamma_{2M}^{-1}\, \tilde{W}_{2M}) \\ & + tr(\tilde{W}_{1C}^T\, \Gamma_{1C}^{-1}\, \tilde{W}_{1C}) + tr(\tilde{W}_{2C}^T\, \Gamma_{2C}^{-1}\, \tilde{W}_{2C}) \\ & + tr(\tilde{W}_{1G}^T\, \Gamma_{1G}^{-1}\, \tilde{W}_{1G}) + tr(\tilde{W}_{2G}^T\, \Gamma_{2G}^{-1}\, \tilde{W}_{2G}) \\ & + tr(\tilde{W}_{1D}^T\, \Gamma_{1D}^{-1}\, \tilde{W}_{1D}) + tr(\tilde{W}_{2D}^T\, \Gamma_{2D}^{-1}\, \tilde{W}_{2D})\;), \end{aligned} \tag{47}$$

with the diagonal constant matrices $\Gamma_{\{1,2\}\{M,C,G,D\}}$

$$\begin{array}{ll} \Gamma_{1M} \in \mathbb{R}^{n^2 \times n^2}, & \Gamma_{2M} \in \mathbb{R}^{n\, p_M \times n\, p_M}, \\ \Gamma_{1C} \in \mathbb{R}^{2n^2 \times 2n^2}, & \Gamma_{2C} \in \mathbb{R}^{n\, p_C \times n\, p_C}, \\ \Gamma_{1G} \in \mathbb{R}^{n \times n}, & \Gamma_{2G} \in \mathbb{R}^{p_G \times p_G}, \\ \Gamma_{1D} \in \mathbb{R}^{n \times n}, & \Gamma_{2D} \in \mathbb{R}^{p_D \times p_D}, \end{array} \tag{48}$$

and[6]

$$V_3 = \frac{\lambda_{min}(K)}{2}\, \tilde{\theta}^T \Gamma_\theta^{-1}\, \tilde{\theta}. \tag{49}$$

The function V_1 are differentiating with respect to time

$$\dot{V}_1 = s^T M\, \dot{s} + \frac{1}{2}\, s^T \dot{M}\, s. \tag{50}$$

The proposed control law (23) is used in the dynamic model (19) to obtain the dynamic equation of the variable s

$$M\, \dot{s} + C\, s = \xi - u_{SM}. \tag{51}$$

The application of the property 2 on the equation (51) gives

$$\dot{V}_1 = s^T (M\, \dot{s} + C\, s) = s^T (\xi - u_{SM}). \tag{52}$$

After some calculations of the term $s^T \xi$ using the equation (41)[7], the

[5]The function $tr(x)$ represent the trace of matrix x.
[6]The function $\lambda_{min}(x)$ represent the minimal eigenvalue of the matrix x.
[7]The equality $x^T y = tr(y\, x^T)$ is verified for $\forall x, y \in \mathbb{R}^n$.

derivative of the function V_1 (52) can be rewritten as

$$\begin{aligned}\dot{V}_1 = \; & s^T(Z - u_{SM}) \\ & + tr(\tilde{W}_{1M}^T X_M \ddot{q}_r s^T \hat{W}_{2M}^T \acute{\hat{\Phi}}_M) + tr(\tilde{W}_{2M}^T (\hat{\Phi}_M - \acute{\hat{\Phi}}_M \hat{W}_{1M}^T X_M) \ddot{q}_r s^T) \\ & + tr(\tilde{W}_{1C}^T X_C \dot{q}_r s^T \hat{W}_{2C}^T \acute{\hat{\Phi}}_C) + tr(\tilde{W}_{2C}^T (\hat{\Phi}_C - \acute{\hat{\Phi}}_C \hat{W}_{1C}^T X_C) \dot{q}_r s^T) \\ & + tr(\tilde{W}_{1G}^T X_G s^T \hat{W}_{2G}^T \acute{\hat{\Phi}}_G) + tr(\tilde{W}_{2G}^T (\hat{\Phi}_G - \acute{\hat{\Phi}}_G \hat{W}_{1C}^T X_G) s^T) \\ & + tr(\tilde{W}_{1D}^T X_D s^T \hat{W}_{2D}^T \acute{\hat{\Phi}}_G) + tr(\tilde{W}_{2D}^T (\hat{\Phi}_D - \acute{\hat{\Phi}}_D \hat{W}_{1D}^T X_D) s^T).\end{aligned} \tag{53}$$

Differentiating V_2 with respect to time, to obtain

$$\begin{aligned}\dot{V}_2 = \; & -tr(\tilde{W}_{1M}^T \Gamma_{1M}^{-1} \dot{\hat{W}}_{1M}) - tr(\tilde{W}_{2M}^T \Gamma_{2M}^{-1} \dot{\hat{W}}_{2M}) \\ & - tr(\tilde{W}_{1C}^T \Gamma_{1C}^{-1} \dot{\hat{W}}_{1C}) - tr(\tilde{W}_{2C}^T \Gamma_{2C}^{-1} \dot{\hat{W}}_{2C}) \\ & - tr(\tilde{W}_{1G}^T \Gamma_{1G}^{-1} \dot{\hat{W}}_{1G}) - tr(\tilde{W}_{2G}^T \Gamma_{2G}^{-1} \dot{\hat{W}}_{2G}) \\ & - tr(\tilde{W}_{1D}^T \Gamma_{1D}^{-1} \dot{\hat{W}}_{1D}) - tr(\tilde{W}_{2D}^T \Gamma_{2D}^{-1} \dot{\hat{W}}_{2D}).\end{aligned} \tag{54}$$

The function V_3 are derivative with respect to time

$$\dot{V}_3 = -\lambda_{min}(K) \tilde{\theta}^T \Gamma_\theta^{-1} \dot{\hat{\theta}} = -\lambda_{min}(K) \tilde{\theta}^T \Psi(q, \dot{q}, \dot{q}_r, \ddot{q}_r, \hat{W}) ||s||. \tag{55}$$

The following adaption laws are proposed to obtain $\dot{V}_1 = s^T(Z - u_{SM}) - \dot{V}_2$

$$\begin{cases} \dot{\hat{W}}_{1M} = \Gamma_{1M} X_M \ddot{q}_r s^T \hat{W}_{2M}^T \acute{\hat{\Phi}}_M \\ \dot{\hat{W}}_{2M} = \Gamma_{2M} (\hat{\Phi}_M - \acute{\hat{\Phi}}_M \hat{W}_{1M}^T X_M) \ddot{q}_r s^T \\ \dot{\hat{W}}_{1C} = \Gamma_{1C} X_C \dot{q}_r s^T \hat{W}_{2C}^T \acute{\hat{\Phi}}_C \\ \dot{\hat{W}}_{2C} = \Gamma_{2C} (\hat{\Phi}_C - \acute{\hat{\Phi}}_C \hat{W}_{1C}^T X_C) \dot{q}_r s^T \\ \dot{\hat{W}}_{1G} = \Gamma_{1G} X_G s^T \hat{W}_{2G}^T \acute{\hat{\Phi}}_G \\ \dot{\hat{W}}_{2G} = \Gamma_{2G} (\hat{\Phi}_G - \acute{\hat{\Phi}}_G \hat{W}_{1G}^T X_G) s^T \\ \dot{\hat{W}}_{1D} = \Gamma_{1D} X_D s^T \hat{W}_{2D}^T \acute{\hat{\Phi}}_D \\ \dot{\hat{W}}_{2D} = \Gamma_{2D} (\hat{\Phi}_D - \acute{\hat{\Phi}}_D \hat{W}_{1D}^T X_D) s^T \end{cases} \tag{56}$$

The application of the adaption laws (56) to the derivative of Lyapunov function (45) gives

$$\dot{V} = s^T(Z - u_{SM}) - \lambda_{min}(K) \tilde{\theta}^T \Psi(q, \dot{q}, \dot{q}_r, \ddot{q}_r, \hat{W}) ||s||. \tag{57}$$

The torque u_{SM} (25) is used in (57) to get

$$\dot{V} = s^T(Z - \hat{\theta}^T\Psi(s,\hat{W})\,K\,\frac{s}{||s||}) - \lambda_{min}(K)\,\tilde{\theta}^T\,\Psi(q,\dot{q},\dot{q}_r,\ddot{q}_r,\hat{W})\,||s||. \quad (58)$$

From (58), it could be establised that the derivative of the Lyapunov function verifies the following inequality:

$$\begin{aligned}\dot{V} &\leq s^T Z - \hat{\theta}^T\Psi(s,\hat{W})\,\lambda_{min}(K)\,||s|| - \lambda_{min}(K)\,\tilde{\theta}^T\,\Psi(q,\dot{q},\dot{q}_r,\ddot{q}_r,\hat{W})\,||s|| \\ &\leq s^T Z - \theta^T\Psi(q,\dot{q},\dot{q}_r,\ddot{q}_r,\hat{W})\,\lambda_{min}(K)\,||s|| \\ &\leq ||s||\,(\,||Z|| - \theta^T\Psi(q,\dot{q},\dot{q}_r,\ddot{q}_r,\hat{W})\,\lambda_{min}(K)).\end{aligned} \quad (59)$$

From the inequality (44), it could be obtain $\theta_i > (c_{Zi} + \mu)/\lambda_{min}(K)$ for $i = 1, ..., 8$ so the following inequality is verified:

$$||Z|| - \theta^T\Psi(q,\dot{q},\dot{q}_r,\ddot{q}_r,\hat{W})\,\lambda_{min}(K) < -\mu. \quad (60)$$

Using (60) in (59), it gives

$$\dot{V} < -\mu\,||s||\ . \quad (61)$$

Finally, it can be established that the variables s and $\tilde{W}_{1N}$ and $\tilde{W}_{2N}$ are bounded since $V(t) \geq 0$ and $\dot{V}(t) \leq 0$. In addition, assumptions 3 and 4 allow to guarantee that $\dot{e}$ is uniformly continuous since $\ddot{q}_d$ and $\dddot{q}$ are bounded. As a result, the variable s given in (13) is also uniformly continuous. On the other hand, it can be easily verified from (61) that $\lim_{t\to+\infty}\int_{t_0}^{t}\|s(\mu)\|d\mu \leq \frac{V(t_0)}{\mu}$. Application of Barbalat's lemma [28] indicates that $\lim_{t\to+\infty}\|s(t)\| = 0$. According to the stability performances of the used switching variable s, it can be conclude that $e \to 0$ and $\dot{e} \to 0$ as $t \to +\infty$. Therefore, the proposed controller guarantees a zero steady-state tracking error of the position and velocity trajectories.

5. Experimental validation

5.1. Experimental context

Experimental tests are presented in order to show the effectiveness of the proposed adaptive controller. A Exoskeleton achieve rehabilitation movements without and with three subjects. The used right upper limb exoskeleton called ULEL (Upper Limb Exoskeleton of LISSI) of the LISSI (Laboratoire Image Signaux et Systèmes Intelligents) of Paris Est Creteil University (UPEC) in France, is developed by the company RB3D (see figure 2).

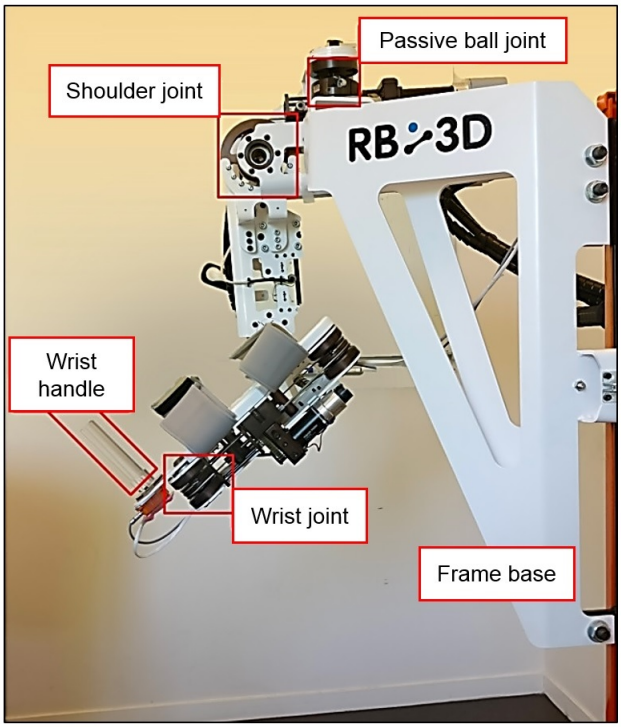

Figure 2: ULEL's joints

ULEL is a right upper limb exoskeleton of 3 DOF (shoulder, elbow and wrist).In this experimentation, the two first joints, shoulder and elbow, are chosen to validate the proposed control. These two joints move in the same plan (see figure 3).

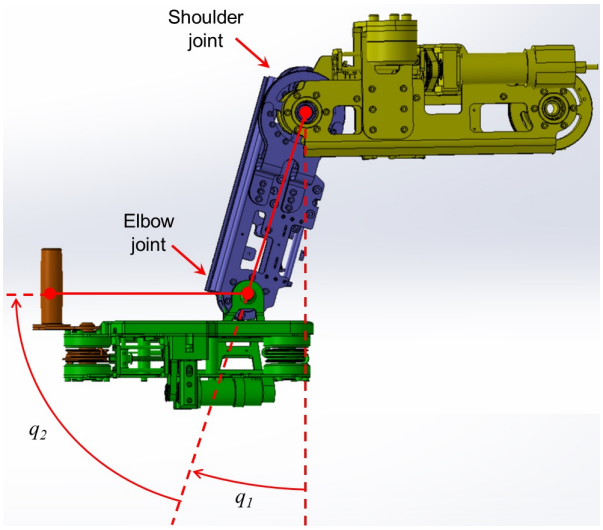

Figure 3: ULEL's Mechanical representation

The two joints are actuated by DC motors of MAXON company, which are current controlled by adequate power cards (Epsos 2) of the same company. The resolution of the nonlinear differential equation of the proposed controller is applied by using the fourth order Runge-Kutta's solver with a sampling time of $10^{-3}sec$. The figure 4 shows our experimental setup based on a computer equipped with a dSpace DS1103 PPC real time controller card. The used software is Matlab/Simulink and dSpace Control Desk software. The real position of each joints are measured by encoders. Low pass filter are used to improve the signal-to-noise ratio and maintain a good transmission. The safety and security requirement were respected during the tests: limit switches, current limit and mechanical stop.

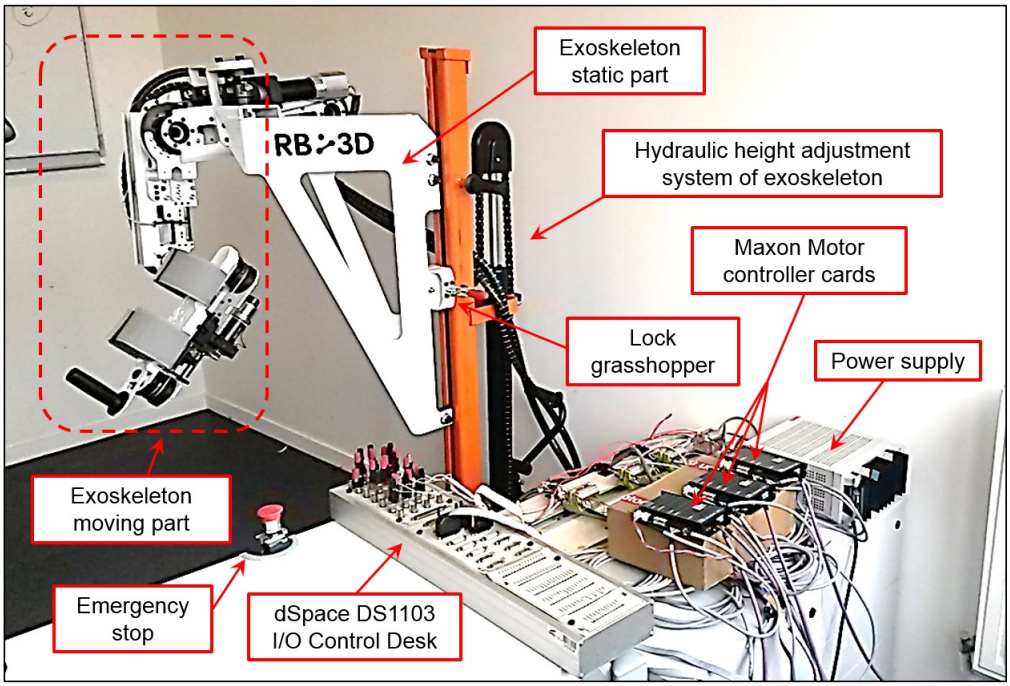

Figure 4: ULEL's protocol of experimentation

5.2. Experimental protocol

Two healthy subjects, the characteristics given in table 1, have being chosen to test the controller. During the tests, ULEL moves the right upper limb of the subjects, which remain passive without applying any assistive or resistive torque. The controller has been also tested on the exoskeleton alone.

Subject	n°1	n°2
Sex	Male	Male
Age	44 years	26 years
Weight	72 kg	95 kg
Height	1.69 m	1.88 m

Table 1: The experimentation subjects.

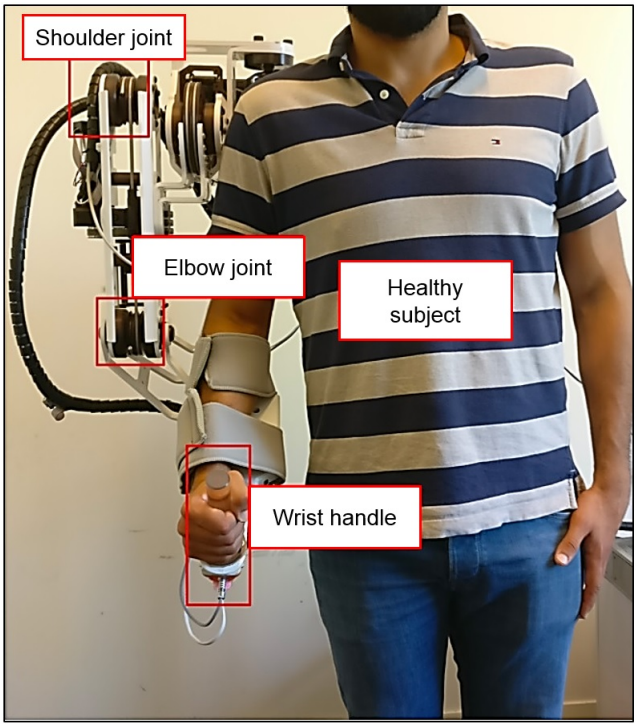

Figure 5: ULEL with a subject

In the experimentation, the term $\frac{s}{||s||+\delta}$ is used in place of the term $s/\left\|s\right\|$ in the equation (25) to avoid chattering of the discontinuous part of sliding control input

$$u_{SM} = \hat{\theta}^T \Psi(q, \dot{q}, \dot{q}_r, \ddot{q}_r, \hat{W})\, K\, \frac{s}{||s|| + \delta}, \tag{62}$$

where $\delta = 0.2$.

The adaptation of all parameters, $\hat{W}_{\{1,2\}\{M,C,G,D\}}$ and $\hat{\theta}$, will be stop when a tolerance threshold is reached: when $||s||$ is lower than δ.

The downwards rest position are chosen like the zero posture of ULEL. The kinematic scheme is given in figure 3. The desired trajectories are defined as $q_{di}(t) = A_i + B_i\, sin(\omega_i t + \varphi_i)$, where i refers to thei^{th} joint, $A_1 = \frac{\pi}{10}\, rad$, $A_2 = \frac{\pi}{4}\, rad$, $B_1 = B_2 = \frac{\pi}{10}\, rad$, $\omega_1 = 0.4\, rad/s$, $\omega_2 = 0.5\, rad/s$, $\varphi_1 = 0\, rad$ and $\varphi_2 = -\frac{\pi}{2}\, rad$. The real initial position and velocity are given by $q(0) = \left[0, \frac{\pi}{4}\right]^T$ and $\dot{q}(0) = [0, 0]^T$. For the adaptive neural networks, all synaptic weight estimations $\hat{W}_{\{1,2\}\{M,C,G,D\}}$ are initialized to zero. The adaptation

matrices $\Gamma_{\{1,2\}\{M,C,G,D\}}$ are equal to $2I$ where I is the identity matrix with appropriate dimension. The used sigmoidal activation function is given by $\sigma : x \mapsto \frac{1}{1+e^{-x}}$.

The sliding mode parameters are chosen: $\gamma_1 = \frac{5}{9}$, $\gamma_2 = \frac{5}{7}$ and $\alpha_i = 1$, $\beta_i = 2$ for $i = 1, 2$. The figure 6 shows some simulation examples of transient convergence obtained by solving the sliding mode differential equation $s_i = 0$ with different initial conditions $q_i(0)$ and with $\dot{q}_i(0)$=0. It can be seen from this figure that the response time is about 5 seconds. The trajectories are smooth and do not exhibit any undesirable variations. This dynamic behavior corresponds to the choice of the used parameters of the sliding surface.

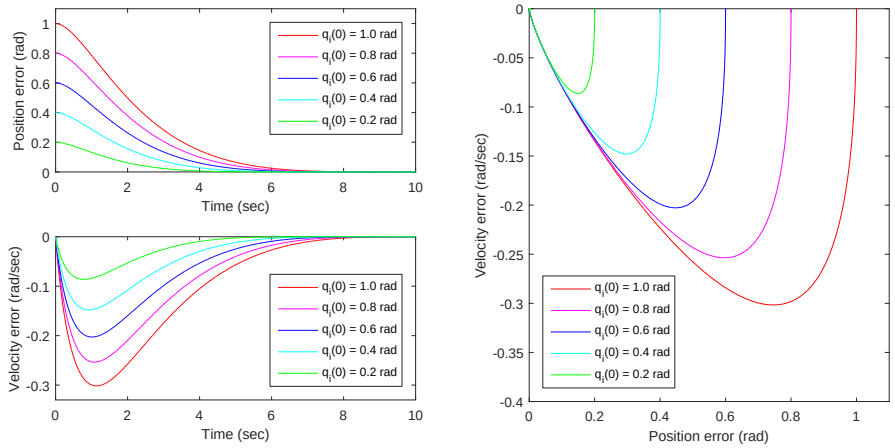

Figure 6: Examples of transient convergence in the sliding mode.

5.3. Experimental result

The figures 7 and 9 show for the three cases (exoskeleton in a standalone mode, exoskeleton with subjects 1 and 2) the desired and the real joint positions and velocities. For all cases, despite of the different wearer morphology, the controller tracks the desired trajectories successfully. Indeed, the real trajectories follow the desired trajectories with errors close to zero. The initial positions of the exoskeleton (at t = 0 sec.) were chosen to be different from the desired trajectories to test the transitional behavior of the closed-loop

system. The results show that during the first few seconds (about 5 sec.) the trajectory of the position is smooth, with no abrupt variations that could be harmful to the human body. This smooth variation is achieved by the choice of the sliding surface proposed in equation (13). The figures 8 and 10 show respectively the tracking errors in position and velocity. it can be seen that the transient response characteristics (shape and response time), provided by the chosen sliding surface $s = 0$, are practically invariant for the three cases shown: without subject, with subject 1 and with subject 2. The forms and response times of the tracking errors are in compliance with the responses obtained in the figure 6.

The control inputs are showed in the figure 11. The impact of the subject's morphology on the required control torque for each joint could be noted. The torque amplitudes increase with the subject's weight and height. The chattering reduced by using the small parameter δ in the equation (62) makes the applied torques acceptable for rehabilitation exercises. The small excitations in high frequency are what remains of the theoretical chattering of the sliding mode control. The remainder of the observed chattering is permissible and did not cause any damage to the actuator. It is also found that the stability of the system is not affected by this phenomenon.

It can be seen from the figure 12 that after a short moment, the norm of the sliding surface s become lower than the threshold.

To show the contribution of the two parts u_{NN} and u_{SM} in the control, the case of the subject 2 (the heavier) has been chosen and shown in the figure 13. The torques u_{NN} start at zero, because of the initialization of all synaptic weight estimations at zero. During this beginning phase, the control is ensured by the sliding mode parts u_{SM}. After the adaptation period, a stable steady state is reached by the torques u_{NN}.

The figures 14 and 15 show than the parameters $\hat{W}_{\{1,2\}\{M,C,G,D\}}$ and $\hat{\theta}$ stop their adaptation when the norm of s is less than the threshold δ (see figure 12).

The steady states of the norms $||\hat{W}||_F$ are depending of the subject show clearly in the figures 14. Like for the torques, a link between the amplitude of the norms and the subject's weight and height can be noted.

The evolution of adaptive parameters $\hat{\theta} = [\hat{\theta}_1, ..., \hat{\theta}_8]^T$ is showed in the figure 15. The estimates parameters $\hat{\theta} = [\hat{\theta}_1, ..., \hat{\theta}_8]^T$ start at zero, as the initial values of all parameters are set to 0 at the initialisation phase, and converge to the a stable value during the adaptation phase.

Finally, the experimental results show clearly the robustness and the tracking performance effectiveness of the proposed controller. It can be noted that the practical implementation of the proposed controller requires a sufficiently powerful and fast control card to support the calculations of the used nonlinear models. The computation time set at a sampling constant equal to 0.001 seconds is sufficient and do not cause any unwanted effects on human subjects.

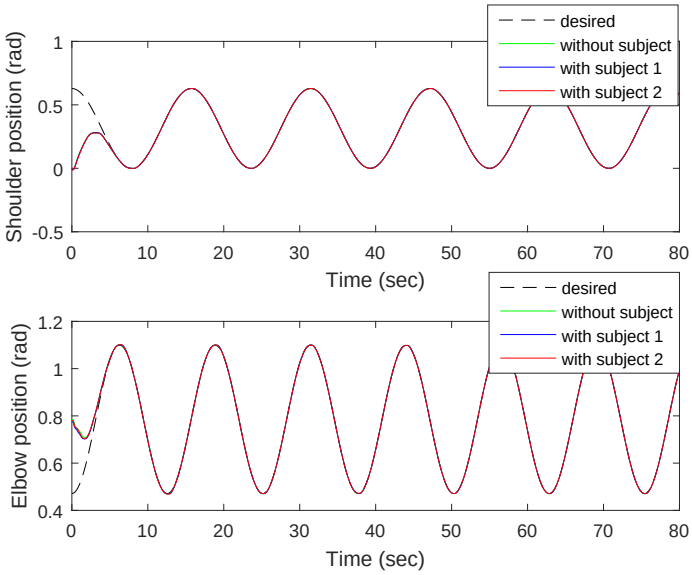

Figure 7: The positions of the two joints.

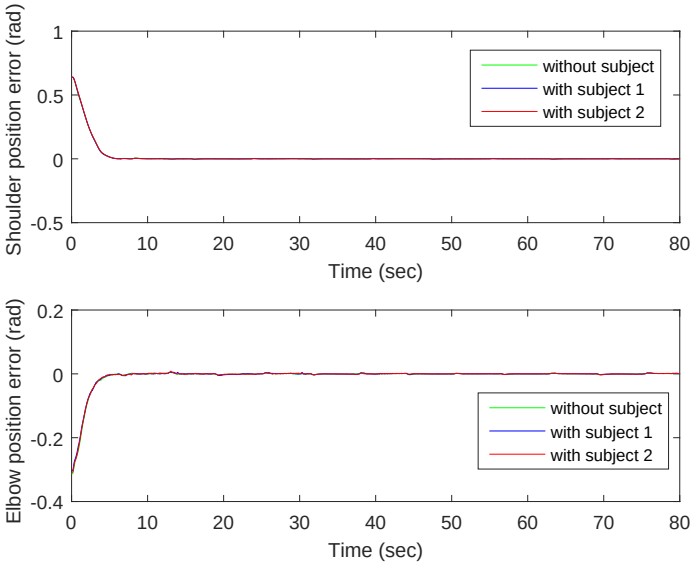

Figure 8: The position errors of the two joints.

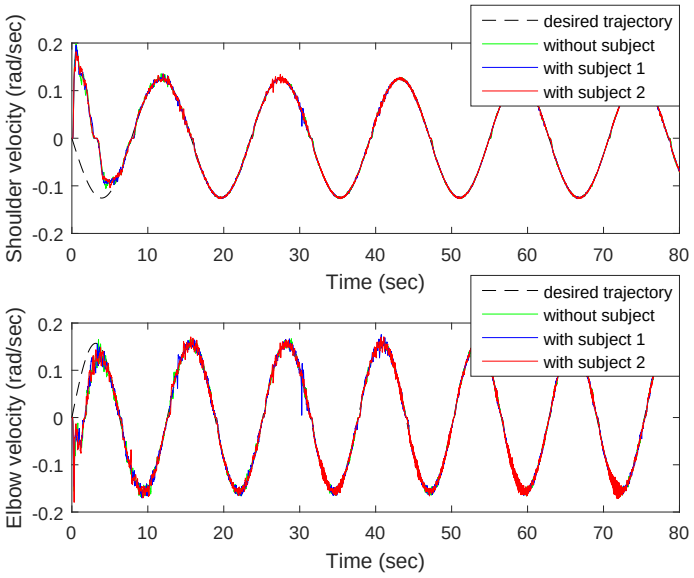

Figure 9: The velocities of the two joints.

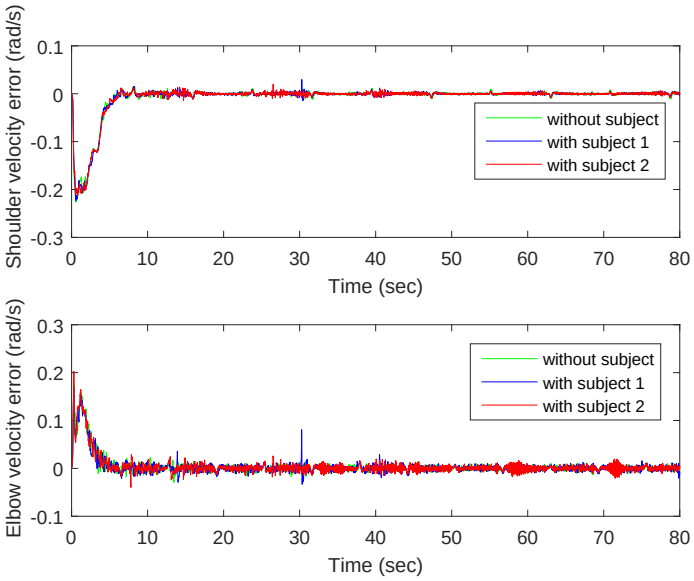

Figure 10: The velocity errors of the two joints.

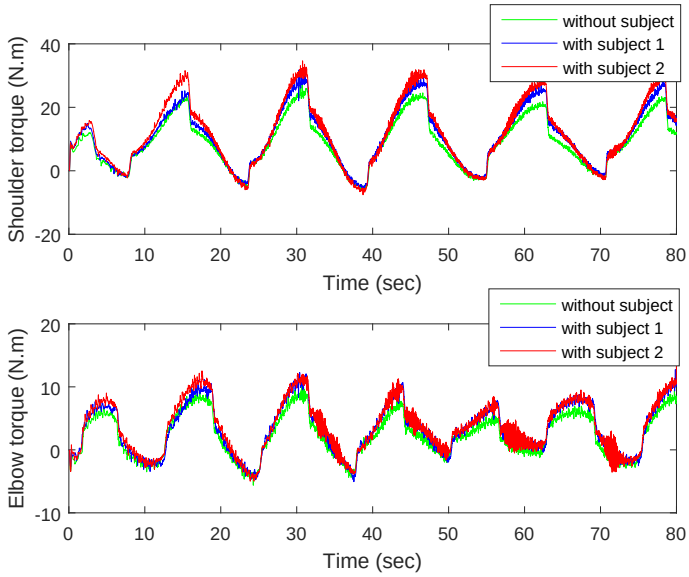

Figure 11: The torques of the two joints.

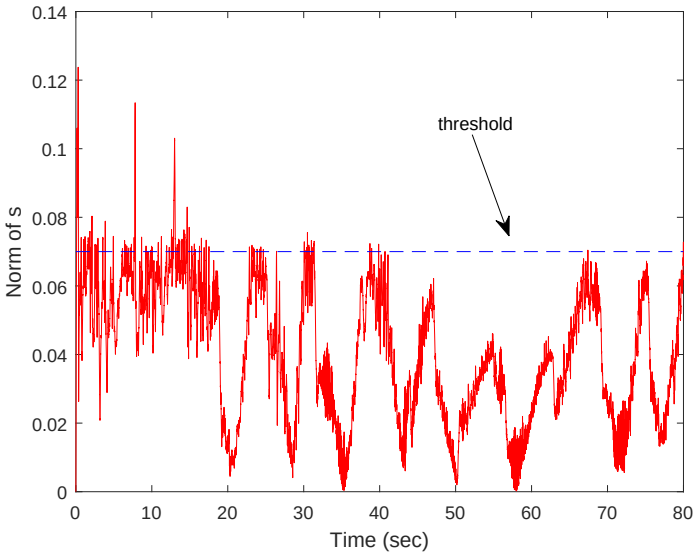

Figure 12: The norm $||s||$ for the subject 2.

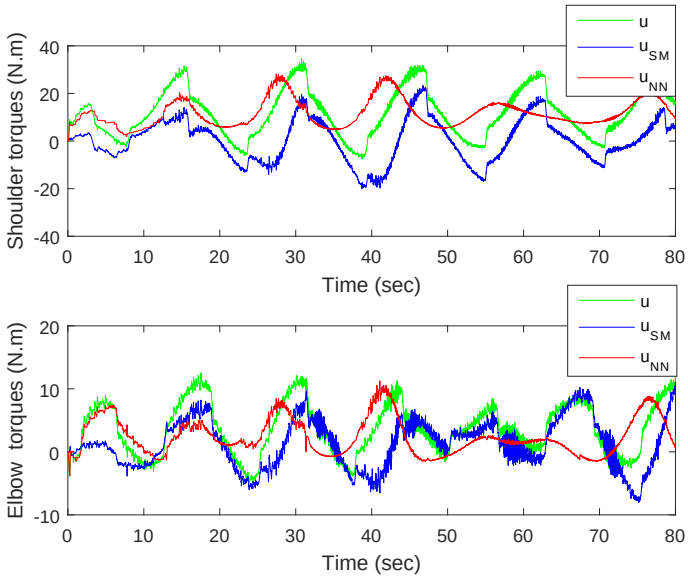

Figure 13: The torques u_{SM} and u_{NN} for subject 2.

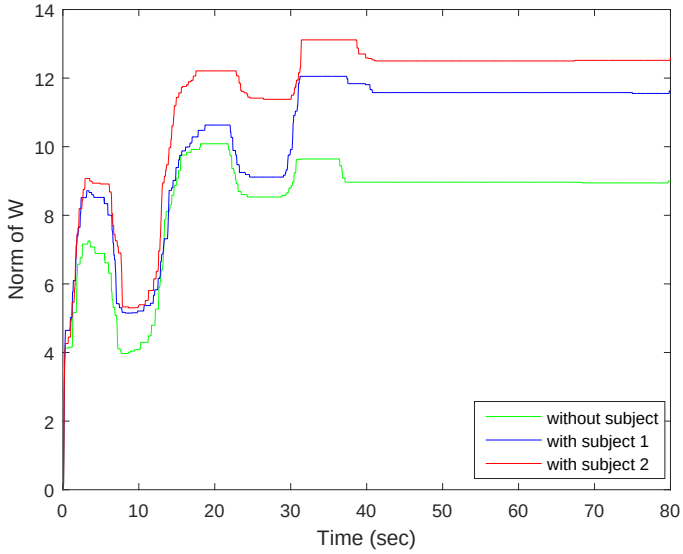

Figure 14: The evolution of $||\hat{W}||_F$.

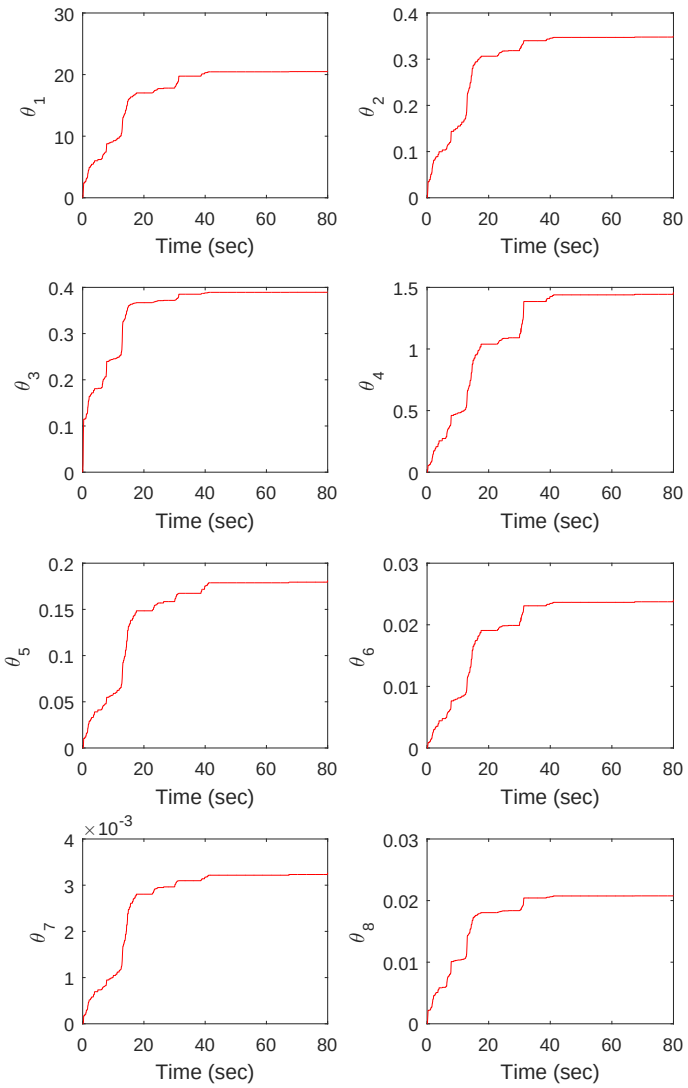

Figure 15: The estimation of θ for the subject 2.

6. Conclusion

This paper presents a new adaptive controller for trajectory tracking of exoskeletons with uncertain model errors and external disturbances. This approach uses a combination of a continuous NN and a discontinuous SM controller. The continuous NN part approximates the dynamic model of the exoskeleton-human system, which depends on the wearer and his morphology. Robustness to disturbances and approximation errors is ensured by the SM part. Consequently, this approach does not require the knowledge of the exact system dynamic model since only some parameter bounds are assumed to be known. Stability has been proven by the use of Lyapunov's theorem and verified experimentally. The results of the real-time application on 2-DOF exoskeleton showed the effectiveness of the proposed controller and its satisfactory performances for different subjects characteristics. Finally, since the proof using Lyapunov's theorem demonstrates only asymptotic convergence of the state variables, the finite time convergence could be investigated in future work.

References

[1] J. C. Perry and J. Rosen, "Design of a 7 degree-of-freedom upper-limb powered exoskeleton," in *The First IEEE/RAS-EMBS International Conference on Biomedical Robotics and Biomechatronics, 2006. BioRob 2006.*, Feb 2006, pp. 805–810.

[2] R. Riener, "Technology of the robotic gait orthosis lokomat," in *Neurorehabilitation Technology*. Springer, 2016, pp. 395–407.

[3] J. F. Veneman, R. Kruidhof, E. E. Hekman, R. Ekkelenkamp, E. H. Van Asseldonk, and H. Van Der Kooij, "Design and evaluation of the lopes exoskeleton robot for interactive gait rehabilitation," *IEEE Transactions on Neural Systems and Rehabilitation Engineering*, vol. 15, no. 3, pp. 379–386, 2007.

[4] W. Yu and J. Rosen, "A novel linear pid controller for an upper limb exoskeleton," in *Decision and Control (CDC), 2010 49th IEEE Conference on*. IEEE, 2010, pp. 3548–3553.

[5] T. Madani, B. Daachi, and K. Djouani, "Non-singular terminal sliding mode controller: Application to an actuated exoskeleton," *Mechatronics*, vol. 33, pp. 136–145, 2016.

[6] E. E. Cavallaro, J. Rosen, J. C. Perry, and S. Burns, "Real-time myoprocessors for a neural controlled powered exoskeleton arm," *IEEE Transactions on Biomedical Engineering*, vol. 53, no. 11, pp. 2387–2396, 2006.

[7] F. Girosi and T. Poggio, "Networks and the best approximation property," *Biological cybernetics*, vol. 63, no. 3, pp. 169–176, 1990.

[8] T. H. Lee and C. J. Harris, *Adaptive neural network control of robotic manipulators*. World Scientific, 1998, vol. 19.

[9] S. S. Ge and C. C. Hang, "Direct adaptive neural network control of robots," *International journal of systems science*, vol. 27, no. 6, pp. 533–542, 1996.

[10] M.-D. Tran and H.-J. Kang, "Adaptive terminal sliding mode control of uncertain robotic manipulators based on local approximation of a dynamic system," *Neurocomputing*, vol. 228, pp. 231–240, 2017.

[11] B. Achili, T. Madani, B. Daachi, and K. Djouani, "Adaptive observer based on mlpnn and sliding mode for wearable robots: Application to an active joint orthosis," *Neurocomputing*, vol. 197, pp. 69–77, 2016.

[12] V. I. Utkin, "Sliding modes and their applications in variable structure systems," *Mir, Moscow*, 1978.

[13] M. Zhihong, A. P. Paplinski, and H. R. Wu, "A robust mimo terminal sliding mode control scheme for rigid robotic manipulators," *IEEE transactions on automatic control*, vol. 39, no. 12, pp. 2464–2469, 1994.

[14] X. Yu and M. Zhihong, "Fast terminal sliding-mode control design for nonlinear dynamical systems," *IEEE Transactions on Circuits and Systems I: Fundamental Theory and Applications*, vol. 49, no. 2, pp. 261–264, 2002.

[15] Y. Feng, X. Yu, and Z. Man, "Non-singular terminal sliding mode control of rigid manipulators," *Automatica*, vol. 38, no. 12, pp. 2159–2167, 2002.

[16] H. Komurcugil, "Non-singular terminal sliding-mode control of dc-dc buck converters," *Control Engineering Practice*, vol. 21, no. 3, pp. 321 – 332, 2013.

[17] L. Peng, M. Jianjun, G. Lina, and Z. Zhiqiang, "Integral terminal sliding mode control for uncertain nonlinear systems," in *Control Conference (CCC), 2015 34th Chinese*. Hangzhou, China: IEEE, 2015, pp. 824–828.

[18] A. Riani, T. Madani, A. Benallegue, and K. Djouani, "Adaptive integral terminal sliding mode control for upper-limb rehabilitation exoskeleton," *Control Engineering Practice*, vol. 75, pp. 108 – 117, 2018.

[19] A. Jebri, T. Madani, and K. Djouani, "Adaptive continuous integral-sliding-mode controller for wearable robots: Application to an upper limb exoskeleton," in *2019 IEEE 16th International Conference on Rehabilitation Robotics (ICORR)*, June 2019, pp. 766–771.

[20] W. Khalil and E. Dombre, *Modeling, identification and control of robots*. Oxford: Butterworth-Heinemann, 2004.

[21] M. Spong, S. Hutchinson, and M. Vidyasagar, *Robot Modeling and Control*. New York, USA: Wiley, 2006.

[22] F. Ghorbel, B. Srinivasan, and M. W. Spong, "On the uniform boundedness of the inertia matrix of serial robot manipulators," *Journal of Robotic Systems*, vol. 15, no. 1, pp. 17–28, 1998.

[23] C. Kwan, D. Dawson, and F. Lewis, "Robust adaptive control of robots using neural network: global tracking stability," in *Decision and Control, 1995., Proceedings of the 34th IEEE Conference on*, vol. 2. IEEE, 1995, pp. 1846–1851.

[24] D. Y. Meddah and A. Benallegue, "A stable neuro-adaptive controller for rigid robot manipulators," *Journal of Intelligent and Robotic Systems*, vol. 20, no. 2-4, pp. 181–193, 1997.

[25] B. Daachi and A. Benallegue, "A stable neural adaptive force controller for a hydraulic actuator," *Proceedings of the Institution of Mechanical Engineers, Part I: Journal of Systems and Control Engineering*, vol. 217, no. 4, pp. 303–310, 2003.

[26] A. Riani, "Commande et observation des exosquelettes pour la rééducation fonctionnelle du membre supérieur," Ph.D. dissertation, Université Paris-Saclay, 2018.

[27] T. Madani, B. Daachi, and K. Djouani, "Modular-controller-design-based fast terminal sliding mode for articulated exoskeleton systems," *IEEE Transactions on Control Systems Technology*, vol. 25, no. 3, pp. 1133–1140, 2017.

[28] I. Barbalat, "Systemes d'equations differentielles d'oscillations non lineaires," *Rev. Math. Pures Appl*, vol. 4, no. 2, pp. 267–270, 1959.